ORIGINAL PAPER

Nagoya J. Med. Sci. **86**. 189–200, 2024
doi:10.18999/nagjms.86.2.189

Tissue characteristics of residual lesion in patients with acute coronary syndrome caused by plaque rupture versus plaque erosion: a single-center, retrospective, observational study

Wataru Suzuki, Hirofumi Ohashi, Hirohiko Ando, Yusuke Nakano, Hiroaki Takashima, Masanobu Fujimoto, Hiroaki Sawada, Reiji Goto, Akihiro Suzuki, Shinichiro Sakurai and Tetsuya Amano

Department of Cardiology, Aichi Medical University, Nagakute, Japan

ABSTRACT

Patients with acute coronary syndrome (ACS), frequently caused by plaque rupture (PR), often have vulnerable plaques in residual lesions as well as in culprit lesions. However, whether this occurs in patients with plaque erosion (PE) as well is unknown. We retrospectively analyzed the data of 88 patients with ACS who underwent both optimal coherence tomography (OCT) and intravascular ultrasound (IVUS). Based on plaque morphology of the culprit lesions identified using OCT, patients were classified into PE (n=23) and PR (n=35) groups. The tissue characteristics of residual lesions evaluated using integrated backscatter IVUS were compared between both groups after percutaneous coronary intervention. The PE group had a significantly lower percent lipid volume and a higher percent fibrous volume than the PR group (35.0±17.8% vs 49.2±13.4%, $p<0.001$; 63.2±17.1% vs 50.3±13.1%, $p=0.002$, respectively). Receiver operating characteristic curve analysis revealed that percent lipid volume in the residual lesions was a significant discriminant factor in estimating the plaque morphology of the culprit lesion (optimal cut-off value, <43.5%; sensitivity and specificity values were 73.9% and 68.6%, respectively). In conclusion, patients with PE had a significantly lower percent lipid volume and a significantly higher percent fibrous volume in the residual lesions than those with PR, suggesting that the nature of coronary plaques in patients with PE is different from that of those with PR.

Keywords: plaque rupture, plaque erosion, integrated backscatter intravascular ultrasound, optical coherence tomography, acute coronary syndrome

Abbreviations:
ACS: acute coronary syndrome
IB-IVUS: integrated backscatter intravascular ultrasound
IVUS: intravascular ultrasound
OCT optimal coherence tomography
PE: plaque erosion
PR: plaque rupture

Received: May 12, 2023; accepted: August 8, 2023
Corresponding Author: Hirohiko Ando, MD, PhD
Department of Cardiology, Aichi Medical University, 1-1 Yazakokarimata, Nagakute 480-1195, Japan
Tel: +81-561-62-3311, Fax: +81-561-62-4866, E-mail: anhiro@aichi-med-u.ac.jp

INTRODUCTION

Plaque erosion (PE) is frequently observed as the second most common cause (26–41%) of acute coronary syndrome (ACS) after plaque rupture (PR).[1-5] From a preventive point of view, careful insight into residual lesions in ACS patients could provide a better understanding of preventive strategies because these lesions could also be a substrate for subsequent coronary events.[6,7] While previous intracoronary imaging studies have shown that patients with ACS have vulnerable plaques in residual lesions,[8-11] PR and PE were not considered as separate causes of ACS. Considering PR is the main cause of ACS, the results of these studies might have reflected only the characteristics of PR. It is not well known whether multivessel vulnerability shown in patients having PR also applies to those having PE.

Intravascular ultrasound (IVUS) imaging provides deeper penetration than other intracoronary imaging modalities, such as optical coherence tomography (OCT), resulting in visualization of the entire vessel wall and is currently considered the gold standard to assess coronary plaque tissue characteristics. The addition of an integrated backscatter (IB) technique to IVUS imaging (IB-IVUS) aids in the volumetric assessment of coronary plaque characteristics that has an excellent correlation with histopathological findings.[12] This method has been used in many in vivo clinical studies.[8,13-17] In the present study, we utilized IB-IVUS to evaluate the tissue characteristics of residual lesions in patients with PE and compared them with those in patients with PR.

METHODS

Study population

In this single-center, retrospective, observational study, consecutive patients with ACS who were admitted to the Aichi Medical University (Nagakute, Japan) from September 2017 to July 2019 and underwent both OCT and IVUS were included. Patients with ACS included those who suffered ST-elevation myocardial infarction, non-ST-elevation myocardial infarction, and unstable angina.[18] Patients whose culprit lesion was an in-stent lesion or graft-vessel lesion and those whose OCT or IVUS image quality was poor were excluded. This study was conducted in accordance with the principles of the Declaration of Helsinki established by the World Medical Association. The study protocol was approved by the Ethics Committee of Aichi Medical University (Nagakute, Japan), and all patients provided written informed consent.

OCT examination and imaging analysis

The plaque morphology of the culprit lesions, which were determined based on electrocardiography, echocardiography, and coronary angiography findings, were evaluated using OCT after manual aspiration thrombectomy. Intracoronary images of the culprit lesions were acquired using a frequency-domain OCT system (ILUMIEN OPTIS, Abbott Vascular, Santa Clara, CA, USA or LUNAWAVE, Terumo Corporation, Tokyo, Japan). The technique of OCT image acquisition has been described elsewhere.[19-21] Briefly, OCT catheters (Dragonfly, Abbott Vascular, Santa Clara, CA, USA or FastView, Terumo Corporation, Tokyo, Japan) were advanced distally to the culprit lesion over a 0.014-inch guidewire. The OCT catheter pullbacks were performed during injection of 100% contrast medium from the guiding catheter, acquiring images at a speed of 36 mm/s with the Dragonfly catheter and 40 mm/s with the FastView catheter. The OCT images were analyzed using a dedicated offline review system by two experienced investigators. The plaque morphologies of culprit lesions were classified as PE, PR, calcified nodule, and others on the basis of previously established criteria.[2,5] PE was defined based on the presence of the attached

thrombus overlying an intact and visualized plaque, luminal surface irregularity at the culprit lesion in the absence of thrombus, or attenuation of the underlying plaque by thrombus without superficial lipid or calcification immediately proximal or distal to the site of thrombus. PR was defined according to the presence of fibrous cap discontinuity with communication between the lumen and inner core of the plaque or cavity formation within the plaque. A calcified nodule was identified as a fibrous cap disruption detected over a calcified plaque characterized by protruding calcification, superficial calcium, or the presence of substantive calcium proximal and/or distal to the lesion. Patients who exhibited PE and those who did not were categorized into the PE group and PR group, respectively.

IVUS examination and imaging analysis

After stenting the culprit lesion, IVUS examination of the culprit vessel was performed. The residual lesion was determined as a 5-mm segment located more than 5 mm proximal or 5 mm distal to the stented segment. IVUS imaging data were acquired with a VISICUBE IVUS imaging system using a 60-MHz mechanically rotating IVUS catheter (AltaView, Terumo Corporation, Tokyo, Japan). After the IVUS catheter was advanced distally over a 0.014-inch guidewire, IVUS catheter pullbacks were performed using a motorized pullback device at a speed of 9.0 mm/s. The quantitative measurements of cross-sectional IVUS images were analyzed using manual tracing at 1-mm intervals throughout the lesions. Vessel, lumen, and plaque volumes, calculated using Simpson's method, were standardized as volume index (volume/analyzed length, mm^3/mm). Percent plaque volume was calculated as follows[22]: (plaque volume/vessel volume) × 100, %. The lipid and fibrous characteristics of the residual lesions were also evaluated using IB-IVUS. The IB-IVUS images were analyzed using a computerized offline software (VISIATLAS, Terumo Corporation, Tokyo, Japan). IB values for each tissue characteristic were calculated as the average power of the frequency components of the backscatter signal using a fast Fourier transform, measured in decibels and classified into four color-coded components: blue (lipid), green (fibrous), yellow (dense fibrosis), and red (calcification).[23] The percentage of each tissue characteristic was automatically calculated as follows: (plaque volume/vessel volume) × 100, %.

Statistical analysis

Data were expressed as mean ± standard deviation or as median and interquartile range with differences (95% confidence interval). Categorical variables were expressed as frequencies (%). Continuous variables were compared using the unpaired Student's t-test, and categorical variables were compared using the chi-squared or Fisher's exact test, where appropriate. Mann–Whitney U tests were performed for non-parametric data. Statistical significance was assumed at a p value of 0.05. Receiver operating characteristic curve analysis was performed to assess the optimal cut-off value of percent lipid volume for estimating the plaque morphology of the culprit lesion. The optimal cut-off value was determined using the Youden's index. Differences in the proportion of PE according to percent lipid volume were analyzed using the Cochrane–Armitage trend test. All statistical analyses were performed using IBM SPSS Statistics for Windows, version 22.0 (IBM Corp, Armonk, NY, USA) except for the Cochran–Armitage trend test, which was carried out using R software, version 3.6.1 (R Foundation for Statistical Computing, Vienna, Austria; available as a free download from http://www.r-project.org).

RESULTS

Patient characteristics

A total of 88 patients with ACS were enrolled in the present study (Fig. 1), among whom 22 were excluded because their data could not be analyzed owing to poor OCT (n=17) or IVUS (n=5) images. After excluding 4 patients with calcified nodules and 4 with other morphologies, the data of 23 patients with PE and 35 patients with PR were compared in the present study. There were no significant differences in baseline clinical characteristics between the two groups (Table 1). In terms of the location of culprit lesions, the left anterior descending artery was most frequently affected (69.6%), followed by the right coronary artery (17.4%), whereas in the PR group, the location was equally distributed among the left anterior descending artery and the right coronary artery (48.6% and 42.9%, respectively).

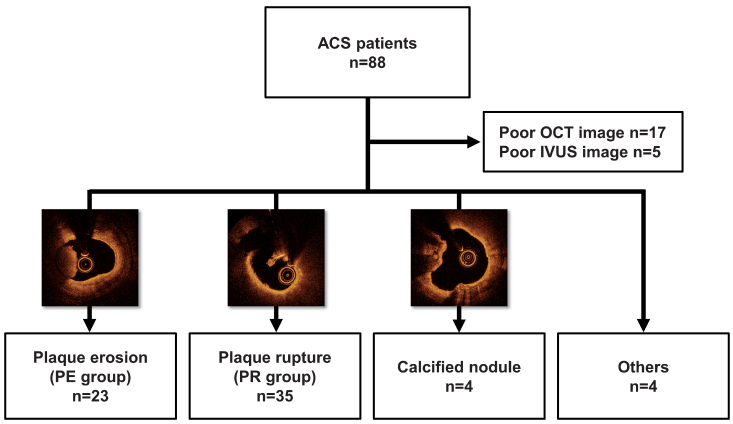

Fig. 1 Study flowchart

ACS: acute coronary syndrome
IVUS: intravascular ultrasound
OCT: optical coherence tomography

Table 1 Patient characteristics

Variable	All patients (n=58)	Plaque erosion (n=23)	Plaque rupture (n=35)	p value
Age, years	67.2±13.8	66.8±14.3	67.4±13.5	0.863
Male sex, n (%)	41 (70.7)	16 (69.6)	25 (71.4)	0.879
BMI, kg/m^2	23.6±3.7	23.5±2.6	23.7±4.4	0.876
Clinical history, n (%)				
Dyslipidemia	30 (51.7)	9 (39.1)	21 (60.0)	0.120
Hypertension	31 (53.4)	9 (39.1)	22 (62.9)	0.076
Smoking	14 (24.1)	4 (17.4)	10 (28.6)	0.305
Diabetes mellitus	19 (32.8)	9 (39.1)	10 (28.6)	0.402
Prior PCI	2 (3.4)	0 (0)	2 (5.7)	0.352

Clinical presentation, n (%)				
STEMI	34 (58.6)	11 (47.8)	23 (65.7)	0.258
NSTE-ACS	24 (41.4)	12 (52.2)	12 (34.3)	
Number of diseased vessels, n (%)				
1 vessel	30 (51.7)	15 (65.2)	15 (42.9)	
2 vessels	22 (37.9)	7 (30.4)	15 (42.9)	0.055
3 vessels	6 (10.3)	1 (4.3)	5 (14.3)	
Target plaque location, n (%)				
Left anterior descending	33 (56.9)	16 (69.6)	17 (48.6)	
Left circumflex	6 (10.3)	3 (13.0)	3 (8.6)	0.349
Right	19 (32.8)	4 (17.4)	15 (42.9)	
Blood lipid levels, mg/dL				
Triglycerides	126.0 [84.0–171.0]	115.5 [82.3–142.5]	149.0 [86.0–177.0]	0.873
HDL cholesterol	46.4±10.6	44.9±9.9	47.7±10.5	0.300
LDL cholesterol	121.9±31.5	115.3±27.0	127.1±33.6	0.150
Medication, n (%)				
Aspirin	8 (13.8)	6 (26.1)	2 (5.7)	0.036
Clopidogrel	3 (5.2)	1 (4.3)	2 (5.7)	0.656
Statins	8 (13.8)	1 (4.3)	7 (20.0)	0.093
Calcium-channel blockers	12 (20.7)	5 (21.7)	7 (20.0)	0.562
Angiotensin-converting enzyme inhibitors	1 (1.7)	0 (0)	1 (2.9)	0.603
Angiotensin II type 1 receptor antagonists	13 (22.4)	3 (13.0)	10 (28.6)	0.165
β-blockers	3 (5.2)	1 (4.3)	2 (5.7)	0.656

Values are presented as mean ± SD, n (%), or median (interquartile range).
BMI: body mass index
PCI: percutaneous coronary intervention
STEMI: ST-elevation myocardial infarction
NSTE-ACS: non-ST elevation-acute coronary syndrome
HDL: high density lipoprotein
LDL: low density lipoprotein

Quantitative parameters in grayscale IVUS and IB-IVUS analyses of residual lesions

The grayscale IVUS analysis of residual lesions showed that vessel volume and plaque volume were significantly smaller in the PE group than in the PR group (64.8±24.1 mm^3 vs 76.2±17.9 mm^3, p=0.042; 20.9±11.1 mm^3 vs 30.7±10.7 mm^3, p=0.01, respectively). IB-IVUS analysis revealed that the percent lipid volume was significantly lower in the PE group than in the PR group (35.0±17.8% vs 49.2±13.4%, p<0.001), whereas the percent fibrous volume was significantly higher in the PE group than in the PR group (63.2±17.1% vs 50.3±13.1%, p=0.002; Table 2). Figure 2 shows representative images of grayscale IVUS and IB-IVUS in residual lesions of the PE and PR groups.

Table 2 Residual lesion analysis using QCA, grayscale IVUS, and IB-IVUS

Variable	Plaque erosion (n=23)	Plaque rupture (n=35)	p value
QCA analysis			
Reference diameter, mm	3.3±0.6	3.3±0.7	0.804
Minimal lumen diameter, mm	3.0±0.6	3.1±0.7	0.783
Percent diameter stenosis, %	8.1±4.4	8.0±5.1	0.925
Grayscale IVUS			
Vessel volume, mm^3	64.8±24.1	76.2±17.9	0.042
Lumen volume, mm^3	43.9±17.4	45.5±12.3	0.672
Plaque volume, mm^3	20.9±11.1	30.7±10.7	0.010
IB-IVUS analysis			
Lipid volume, %	35.0±17.8	49.2±13.4	0.001
Fibrous volume, %	63.2±17.1	50.3±13.1	0.002
Calcification volume, %	1.6±1.7	0.7±0.7	0.032

QCA: quantitative coronary angiography
IVUS: intravascular ultrasound
IB-IVUS: integrated backscatter IVUS

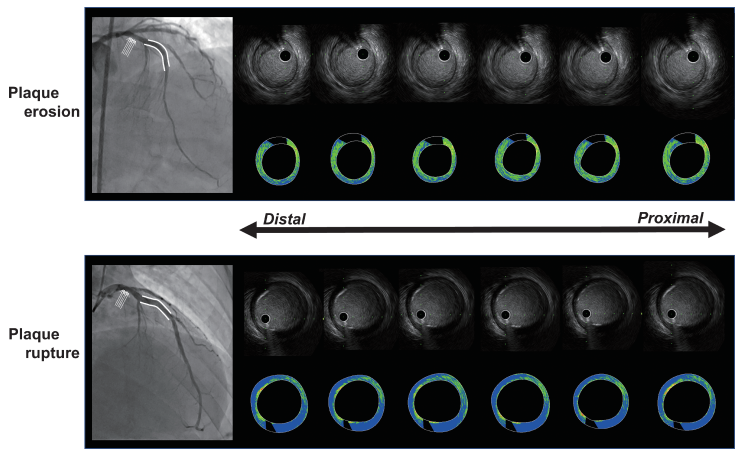

Fig. 2 Representative sequential images of grayscale IVUS and IB-IVUS analyses of residual lesions of the proximal left anterior descending artery
Coronary angiogram showing the location of residual lesions (arrows) and stented culprit lesions (white lines) in the proximal left anterior descending arteries. IB-IVUS showing characteristics of residual lesions. Color-coded components demonstrate lipid (blue), fibrous (green and yellow), and calcification (red). In a patient with PE, the percentages of fibrous volume and lipid volume are 71.5% and 26.3%, respectively. In a patient with PR, the percentages of fibrous volume and lipid volume are 31.6% and 66.7%, respectively.
IVUS: intravascular ultrasound
IB-IVUS: integrated backscatter IVUS
PE: plaque erosion
PR: plaque rupture

Predictive value of residual lesion characteristics for the estimation of culprit lesion morphology

Receiver operating characteristic curve analysis revealed that percent lipid volume in residual lesions was a significant discriminant factor in estimating the plaque morphology of the culprit lesion ($p<0.001$), with an area under the curve of 0.738. The optimal cut-off value of percent lipid volume was <43.5%, and the sensitivity and specificity values were 73.9% and 68.6%, respectively. The proportional analyses stratified according to percent lipid volume in residual lesions showed that the frequency of PE in the culprit lesions increased when the percent lipid volume in the residual lesions decreased ($p<0.001$ for trend; Fig. 3). All the patients with a percent lipid volume <20% in residual lesions exhibited PE in the culprit lesion. In contrast, among patients with percent lipid volume ≥50% in residual lesions, only 21.7% of them demonstrated PE in the culprit lesion (Fig. 4).

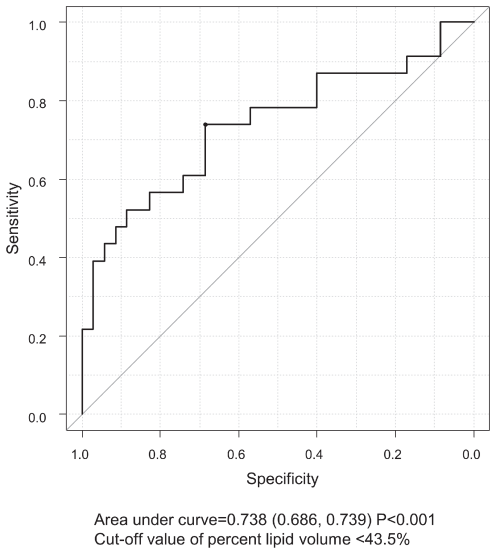

Fig. 3 Predictive value of residual lesion characteristics for estimation of culprit lesion morphology
Receiver operating characteristic curve analysis shows that percent lipid volume in residual lesions is a significant discriminant factor in estimating the plaque morphology of the culprit lesion ($p<0.001$) with an area under the curve (AUC) of 0.738. The optimal cut-off value of percent lipid volume is <43.5%.

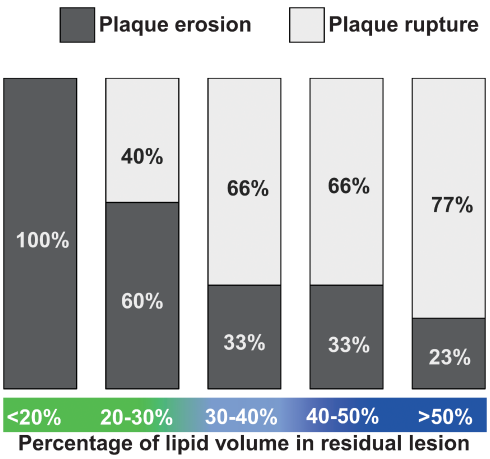

Fig. 4 Relationship between percent lipid volume in residual lesions and the presence of plaque erosion in culprit lesions

According to percent lipid volume in residual lesions, patients are divided into five groups (<20%, 20–30%, 30–40%, 40–50%, and ≥50%). The presence of plaque erosion in the culprit lesion is significantly associated with a lower percent lipid volume in residual lesions (p=0.0011 for trend). All patients with percent lipid volume in residual lesion <20% have plaque erosion in the culprit lesion. In contrast, among patients with percent lipid volume in residual lesion ≥50%, only 21.7% exhibit plaque erosion in the culprit lesion.

DISCUSSION

Our study revealed that the tissue characteristics of residual lesions differed between patients with PE and those with PR. Furthermore, the plaque morphology of the culprit lesions could be estimated based on the plaque characteristics of residual lesions. To the best of our knowledge, this is the first study to evaluate the tissue characteristics of residual lesions in patients with PE.

Tissue characteristics of residual lesions in patients with PE and those with PR

In this study, IB-IVUS analyses demonstrated that patients in the PE group had a lower percent lipid volume and a higher percent fibrous volume in residual lesions than those in the PR group. To date, there are limited data on the characteristics of residual lesions in patients with PE; however, several reports on culprit lesions exist. A previous pathological study has demonstrated that culprit lesions in patients with PE have more fibrous tissue, less necrotic core, and less macrophage infiltration than those in patients with PR.[1] Furthermore, several OCT studies have revealed similar findings regarding the tissue characteristics of culprit lesions in patients with PE; these lesions have lower prevalence of lipid plaque, smaller lipid arc, and less macrophage infiltration than those in patients with PR.[2,5,24] These results suggest that culprit lesions of patients with PE have less plaque vulnerability and less inflammation than those of patients with PR.

Sugiyama et al evaluated the morphological features of residual lesions using OCT in 17 patients with PE.[25] The residual lesions in patients with PE had a lower prevalence of plaque rupture, macrophage accumulation, microvessels, and spotty calcium than those in patients with PR, indicating that patients with PE had lower levels of pancoronary vulnerability than those with PR. The present study, which focused on histological characteristics, rather than morphological characteristics, of residual lesions using IB-IVUS analysis, showed lower lipid tissue and higher fibrous tissue in the PE group, supporting the concept of less inflammation throughout

the coronary tree in patients with PE. Currently, aggressive lipid-lowering therapy is uniformly recommended for all patients with ACS for secondary prevention.[26,27] However, the results of our study suggest that the tissue characteristics of residual lesions differ between patients with PE and those with PR, and the level of plaque vulnerability is lower in patients with PE than those with PR. Therefore, the intensity of lipid-lowering therapy for secondary prevention may need to be individually modified according to the mechanism of ACS and the extent of plaque vulnerability.

Estimation of plaque morphology of culprit lesions using residual lesion characteristics

In the present study, the plaque morphology of culprit lesions could be estimated based on the data regarding residual lesion characteristics obtained using IB-IVUS analyses. Identifying the plaque morphology of the culprit lesion provides useful information about the underlying mechanism of coronary thrombosis.[28-31] The treatment strategy may be changed depending on the underlying mechanism of coronary thrombosis.[32,33] The EROSION study demonstrated that conservative treatment with anti-thrombotic therapy without stenting may be an option for lesions related to PE.[32,33] OCT has been generally used for the in vivo evaluation of plaque morphology of culprit lesions because of its high resolution.[34] However, there are several limitations in using OCT, such as requirement for blood clearance, limited soft tissue penetration, and additional contrast medium use, which often precludes detailed assessment of plaque morphology.[35-37] Moreover, in OCT images, a fresh thrombus sometimes causes a blind spot, especially in cases of ACS, resulting in misdiagnosis of the plaque's morphology.[38] As shown in the present study, assessments of residual lesion characteristics using IB-IVUS might facilitate the diagnosis of plaque morphology of culprit lesions in patients with ACS.

Despite the abovementioned results, the present study has several limitations. First, this was a single-center study involving a relatively small population. The proportion of patients with PE who had a history of hypertension and who took aspirin and statins was smaller than that of patients with PR, which may have affected plaque characteristics. Due to the small size of this study, it was not possible to examine these effects. Therefore, the results are hypothesis-generating. Larger prospective studies are warranted to validate our results. Second, the present study included patients with ACS that is strongly associated with thrombus formation, which might have potentially influenced the results of the IB-IVUS analysis. Third, we defined a residual lesion as a 5-mm segment proximal or distal to the culprit lesion, which comprised only a small part of the entire coronary artery. Therefore, the results of the residual lesion assessment might not reflect the results for all the coronary arteries.

In conclusion, tissue characteristics of residual lesions differed between patients with PE and those with PR. Patients with PE had a significantly lower percent lipid volume and a significantly higher percent fibrous volume in residual lesions compared with those of patients with PR.

ACKNOWLEDGEMENT

The authors would like to thank all the staff and patients who contributed to this study.

DATA AVAILABILITY

The deidentified participant data will not be shared.

CONFLICT OF INTEREST

None.

FINANCIAL SUPPORT

None.

IRB INFORMATION

The study protocol was approved by the Ethics Committee of Aichi Medical University (reference number: 2018-H310).

REFERENCES

1 Virmani R, Kolodgie FD, Burke AP, Farb A, Schwartz SM. Lessons from sudden coronary death: a comprehensive morphological classification scheme for atherosclerotic lesions. *Arterioscler Thromb Vasc Biol.* 2000;20(5):1262–1275. doi:10.1161/01.atv.20.5.1262.

2 Jia H, Abtahian F, Aguirre AD, et al. In vivo diagnosis of plaque erosion and calcified nodule in patients with acute coronary syndrome by intravascular optical coherence tomography. *J Am Coll Cardiol.* 2013;62(19):1748–1758. doi:10.1016/j.jacc.2013.05.071.

3 Higuma T, Soeda T, Abe N, et al. A combined optical coherence tomography and intravascular ultrasound study on plaque rupture, plaque erosion, and calcified nodule in patients with ST-segment elevation myocardial infarction: incidence, morphologic characteristics, and outcomes after percutaneous coronary intervention. *JACC Cardiovasc Interv.* 2015;8(9):1166–1176. doi:10.1016/j.jcin.2015.02.026.

4 Niccoli G, Montone RA, Di Vito L, et al. Plaque rupture and intact fibrous cap assessed by optical coherence tomography portend different outcomes in patients with acute coronary syndrome. *Eur Heart J.* 2015;36(22):1377–1384. doi:10.1093/eurheartj/ehv029.

5 Dai J, Xing L, Jia H, et al. In vivo predictors of plaque erosion in patients with ST-segment elevation myocardial infarction: a clinical, angiographical, and intravascular optical coherence tomography study. *Eur Heart J.* 2018;39(22):2077–2085. doi:10.1093/eurheartj/ehy101.

6 Stone GW, Maehara A, Lansky AJ, et al. A prospective natural-history study of coronary atherosclerosis. *N Engl J Med.* 2011;364(3):226–235. doi:10.1056/NEJMoa1002358.

7 Bae JH, Corban MT, Seo YH, et al. Ten-year clinical outcomes of an intermediate coronary lesion; prognosis and predictors of major adverse cardiovascular events. *Int J Cardiol.* 2020;299:26–30. doi:10.1016/j.ijcard.2019.06.076.

8 Ando H, Amano T, Matsubara T, et al. Comparison of tissue characteristics between acute coronary syndrome and stable angina pectoris–an integrated backscatter intravascular ultrasound analysis of culprit and non-culprit lesions. *Circ J.* 2011;75(2):383–390. doi:10.1253/circj.cj-10-0815.

9 Maejima N, Hibi K, Saka K, et al. Morphological features of non-culprit plaques on optical coherence tomography and integrated backscatter intravascular ultrasound in patients with acute coronary syndromes. *Eur Heart J Cardiovasc Imaging.* 2015;16(2):190–197. doi:10.1093/ehjci/jeu173.

10 Sudo M, Hiro T, Takayama T, et al. Tissue characteristics of non-culprit plaque in patients with acute coronary syndrome vs. stable angina: a color-coded intravascular ultrasound study. *Cardiovasc Interv Ther.* 2016;31(1):42–50. doi:10.1007/s12928-015-0345-1.

11 Pinilla-Echeverri N, Mehta SR, Wang J, et al. Nonculprit lesion plaque morphology in patients with ST-segment-elevation myocardial infarction: results from the complete trial optical coherence tomography substudys. *Circ Cardiovasc Interv.* 2020;13(7):e008768. doi:10.1161/CIRCINTERVENTIONS.119.008768.

12 Kawasaki M, Takatsu H, Noda T, et al. In vivo quantitative tissue characterization of human coronary arterial plaques by use of integrated backscatter intravascular ultrasound and comparison with angioscopic findings. *Circulation.* 2002;105(21):2487–2492. doi:10.1161/01.cir.0000017200.47342.10.

13 Amano T, Matsubara T, Uetani T, et al. Impact of metabolic syndrome on tissue characteristics of angio-

graphically mild to moderate coronary lesions integrated backscatter intravascular ultrasound study. *J Am Coll Cardiol.* 2007;49(11):1149–1156. doi:10.1016/j.jacc.2006.12.028.

14 Amano T, Matsubara T, Uetani T, et al. Impact of omega-3 polyunsaturated fatty acids on coronary plaque instability: an integrated backscatter intravascular ultrasound study. *Atherosclerosis.* 2011;218(1):110–116. doi:10.1016/j.atherosclerosis.2011.05.030.

15 Ando H, Amano T, Takashima H, et al. Differences in tissue characterization of restenotic neointima between sirolimus-eluting stent and bare-metal stent: integrated backscatter intravascular ultrasound analysis for in-stent restenosis. *Eur Heart J Cardiovasc Imaging.* 2013;14(10):996–1001. doi:10.1093/ehjci/jet003.

16 Sakurai S, Takashima H, Waseda K, et al. Influence of plaque characteristics on fractional flow reserve for coronary lesions with intermediate to obstructive stenosis: insights from integrated-backscatter intravascular ultrasound analysis. *Int J Cardiovasc Imaging.* 2015;31(7):1295–1301. doi:10.1007/s10554-015-0699-6.

17 Ando H, Suzuki A, Sakurai S, et al. Tissue characteristics of neointima in late restenosis: integrated backscatter intravascular ultrasound analysis for in-stent restenosis. *Heart Vessels.* 2017;32(5):531–538. doi:10.1007/s00380-016-0903-1.

18 Thygesen K. "Ten Commandments" for the fourth universal definition of myocardial infarction 2018. *Eur Heart J.* 2019;40(3):226. doi:10.1093/eurheartj/ehy856.

19 Tearney GJ, Regar E, Akasaka T, et al. Consensus standards for acquisition, measurement, and reporting of intravascular optical coherence tomography studies: a report from the international working group for intravascular optical coherence tomography standardization and validation. *J Am Coll Cardiol.* 2012;59(12):1058–1072. doi:10.1016/j.jacc.2011.09.079.

20 Prati F, Regar E, Mintz GS, et al. Expert review document on methodology, terminology, and clinical applications of optical coherence tomography: physical principles, methodology of image acquisition, and clinical application for assessment of coronary arteries and atherosclerosis. *Eur Heart J.* 2010;31(4):401–415. doi:10.1093/eurheartj/ehp433.

21 Terada N, Kuramochi T, Sugiyama T, et al. Ventricular fibrillation during optical coherence tomography/optical frequency domain imaging–a large single-center experience. *Circ J.* 2020;84(2):178–185. doi:10.1253/circj.CJ-19-0736.

22 Mintz GS, Garcia-Garcia HM, Nicholls SJ, et al. Clinical expert consensus document on standards for acquisition, measurement and reporting of intravascular ultrasound regression/progression studies. *EuroIntervention.* 2011;6(9):1123–1130. doi:10.4244/EIJV6I9A195.

23 Kawasaki M, Hattori A, Ishihara Y, et al. Tissue characterization of coronary plaques and assessment of thickness of fibrous cap using integrated backscatter intravascular ultrasound–comparison with histology and optical coherence tomography. *Circ J.* 2010;74(12):2641–2648. doi:10.1253/circj.cj-10-0547.

24 Saia F, Komukai K, Capodanno D, et al. Eroded versus ruptured plaques at the culprit site of stemi: In vivo pathophysiological features and response to primary PCI. *JACC Cardiovasc Imaging.* 2015;8(5):566–575. doi:10.1016/j.jcmg.2015.01.018.

25 Sugiyama T, Yamamoto E, Bryniarski K, et al. Nonculprit plaque characteristics in patients with acute coronary syndrome caused by plaque erosion vs plaque rupture: a 3-vessel optical coherence tomography study. *JAMA Cardiol.* 2018;3(3):207–214. doi:10.1001/jamacardio.2017.5234.

26 Grundy SM, Stone NJ, Bailey AL, et al. 2018 AHA/ACC/AACVPR/AAPA/ABC/ACPM/ADA/AGS/APhA/ASPC/NLA/PCNa guideline on the management of blood cholesterol: executive summary: a report of the American College of Cardiology/American Heart Association task force on clinical practice guidelines. *J Am Coll Cardiol.* 2019;73(24):3168–3209. doi:10.1016/j.jacc.2018.11.002.

27 Mach F, Baigent C, Catapano AL, et al. 2019 ESC/EAS guidelines for the management of dyslipidaemias: lipid modification to reduce cardiovascular risk. *Eur Heart J.* 2020;41(1):111–188. doi:10.1093/eurheartj/ehz455.

28 Virmani R, Burke AP, Farb A, Kolodgie FD. Pathology of the vulnerable plaque. *J Am Coll Cardiol.* 2006;47(8 Suppl):C13–C18. doi:10.1016/j.jacc.2005.10.065.

29 Arbab-Zadeh A, Nakano M, Virmani R, Fuster V. Acute coronary events. *Circulation.* 2012;125(9):1147–1156. doi:10.1161/CIRCULATIONAHA.111.047431.

30 Libby P, Pasterkamp G. Requiem for the 'vulnerable plaque'. *Eur Heart J.* 2015;36(43):2984–2987. doi:10.1093/eurheartj/ehv349.

31 Partida RA, Libby P, Crea F, Jang IK. Plaque erosion: a new in vivo diagnosis and a potential major shift in the management of patients with acute coronary syndromes. *Eur Heart J.* 2018;39(22):2070–2076. doi:10.1093/eurheartj/ehx786.

32 Jia H, Dai J, Hou J, et al. Effective anti-thrombotic therapy without stenting: Intravascular optical coherence tomography-based management in plaque erosion (the EROSION study). *Eur Heart J.* 2017;38(11):792–800.

doi:10.1093/eurheartj/ehw381.
33 Xing L, Yamamoto E, Sugiyama T, et al. EROSION study (effective anti-thrombotic therapy without stenting: intravascular optical coherence tomography-based management in plaque erosion): a 1-year follow-up report. *Circ Cardiovasc Interv.* 2017;10(12):e005860. doi:1 0.1161/CIRCINTERVENTIONS.117.005860.
34 Jia H, Kubo T, Akasaka T, Yu B. Optical coherence tomography guidance in management of acute coronary syndrome caused by plaque erosion. *Circ J.* 2018;82(2):302–308. doi:10.1253/circj.CJ-17-1373.
35 Koskinas KC, Ughi GJ, Windecker S, Tearney GJ, Räber L. Intracoronary imaging of coronary atherosclerosis: validation for diagnosis, prognosis and treatment. *Eur Heart J.* 2016;37(6):524–535. doi:10.1093/eurheartj/ehv642.
36 Räber L, Mintz GS, Koskinas KC, et al. Clinical use of intracoronary imaging. Part 1: guidance and optimization of coronary interventions. An expert consensus document of the European Association of Percutaneous Cardiovascular Interventions. *Eur Heart J.* 2018;39(35):3281–3300. doi:10.1093/eurheartj/ehy285.
37 Maehara A, Matsumura M, Ali ZA, Mintz GS, Stone GW. IVUS-guided versus CT-guided coronary stent implantation: a critical appraisal. *JACC Cardiovasc Imaging.* 2017;10(12):1487–1503. doi:10.1016/j.jcmg.2017.09.008.
38 Ando H, Ohashi H, Nakano Y, Takashima H, Amano T. Detailed characterization of vulnerable plaque morphology by high-resolution intravascular ultrasound. *Circ J.* 2020;84(9):1606. doi:10.1253/circj.CJ-20-0355.